

1 Estimating RSV seasonality from 2 pandemic disruptions: a modelling study

3
4 Fabienne Krauer¹, Tor Erlend Fjelde², Mihaly Koltai¹, David Hodgson¹, Marina Treskova-
5 Schwarzbach³, Christine Harvey⁴, Mark Jit¹, Ole Wichmann³, Thomas Harder³, Stefan Flasche¹

6
7 ¹ Centre for Mathematical Modelling of Infectious Diseases, London School of Hygiene &
8 Tropical Medicine, London, UK

9 ² Computational and Biological Learning, Department of Engineering, University of Cambridge,
10 UK

11 ³ Robert Koch Institut, Berlin, Germany

12 ⁴ Health Protection NSW, NSW Ministry of Health

13

14

15 Corresponding author:

16 fabienne.krauer@lshtm.ac.uk

17

18 Abstract

19 **Background:** Respiratory syncytial virus (RSV) is a leading cause of respiratory tract infections
20 and bronchiolitis in young children. The seasonal pattern of RSV is shaped by short-lived
21 immunity, seasonally varying contact rates and pathogen viability. The magnitude of each of
22 these parameters is not fully clear. The disruption of the regular seasonality of RSV during the
23 COVID pandemic in 2020 due to control measures, and the ensuing delayed surge in RSV
24 cases provides an opportunity to disentangle these factors and to understand the implication for
25 vaccination strategies. A better understanding of the drivers of RSV seasonality is key for
26 developing future vaccination strategies.

27 **Methods:** We developed a mathematical model of RSV transmission, which simulates the
28 sequential re-infection (SEIRRS4) and uses a flexible Von Mises function to model the seasonal
29 forcing. Using MCMC we fit the model to laboratory confirmed RSV data from 2010-2022 from
30 NSW while accounting for the reduced contact rates during the pandemic with Google mobility
31 data. We estimated the baseline transmission rate, its amplitude and shape during RSV season
32 as well as the duration of immunity. The resulting parameter estimates were compared to a fit to
33 pre-pandemic data only, and to a fit with a cosine forcing function. We then simulated the
34 expected shifts in peak timing and amplitude under two vaccination strategies: continuous and
35 seasonal vaccination.

36 **Results:** We estimate that RSV dynamics in NSW can be best explained by a high effective
37 baseline transmission rate (2.94/d, 95% CrI 2.72-3.19) and a narrow peak with a maximum 13%
38 increase compared to the baseline transmission rate. We also estimate the duration of post
39 infection temporary but sterilizing immunity to be 412 days (95% CrI 391-434). A cosine forcing

40 resulted in a similar fit and posterior estimates. Excluding the data from the pandemic period in
41 the fit increased parameter correlation and yielded less informative posterior distributions. The
42 continuous vaccination strategy led to more extreme seasonal incidence with a delay in the
43 peak timing and a higher amplitude whereas seasonal vaccination flattened the incidence
44 curves.

45 **Conclusion:** Quantifying the parameters that govern RSV seasonality is key in determining
46 potential indirect effects from immunization strategies as those are being rolled out in the next
47 few years.

48 Introduction

49 Respiratory syncytial virus (RSV) is an endemic virus and a leading cause of acute lower
50 respiratory tract infections in young children. The majority are infected at least once before they
51 are two years old [1]. Subsequent re-infections and infections at older age are thought to result
52 in less severe disease [2,3]. Typical complications of RSV in young children are bronchiolitis or
53 pneumonia. The proportion asymptomatic among infected individuals ranges from 9% in <1
54 year olds to 78% in adults [4].

55
56 To date, the only available measure for pharmaceutical prevention of severe disease is
57 palivizumab, a short-lived and costly monoclonal antibody; no active immunisation product has
58 been licensed yet. Several vaccine candidates and a long-lasting monoclonal antibody are
59 undergoing trials in young infants, pregnant women or the elderly [5,6]. The optimal vaccination
60 strategy depends on the efficacy and duration of immunity conferred [7]. Anticipating short-lived
61 protection from immunisation, seasonal immunisation of infants before the onset of RSV season
62 was estimated to be more cost-effective than year-round vaccination [6,8].

63
64 RSV has a distinct and consistent seasonal pattern in many temperate climate settings [9,10].
65 The regular seasonality is likely an interplay of the seasonal fluctuations in human contacts,
66 meteorological determinants that govern pathogen viability and host susceptibility, as well as the
67 characteristics of the immune response following infection [11–16]. The factors that govern
68 seasonality have been challenging to quantify, and a given seasonal disease pattern may be
69 modelled with various combinations of parameter values. Identifiable and robust parameters are
70 crucial for predicting incidence and determining the potential indirect effects from immunisation
71 strategies as those are being rolled out in the next few years.

72
73 The COVID pandemic, where mobility was restricted globally and contacts were reduced
74 dramatically while seasonal climatic pathogen properties and duration of RSV immunity were
75 unchanged, provides a unique opportunity to estimate the magnitude of the different factors
76 contributing to the regular RSV seasonal pattern observed in temperate settings. The COVID
77 control measures have disrupted the seasonal pattern of RSV around the globe. Countries in
78 the Southern hemisphere, where the initial lockdowns occurred at the beginning of the season,
79 showed an abrupt termination of the 2020 season followed by a delayed peak once the
80 restrictions were eased (see e.g. Australia [17–19] or South Africa [20]). In the Northern
81 hemisphere, the 2020/2021 season following the lockdown period also exhibited a peak delayed

82 by several months in multiple countries (see e.g. France [21], Israel [22], USA [23], Japan [24],
83 UK [25] or Spain [26].

84
85 In this study, we use incident RSV data from New South Wales (NSW, Australia) from sentinel
86 laboratories from 2010-2022 and fit a dynamic transmission model to quantify the magnitude of
87 RSV seasonality and the duration of immunity taking into account the reduction of contacts
88 during the pandemic. We hypothesised that the additional information in the data resulting from
89 the contact reductions facilitates parameter inference by constraining the parameter space. To
90 approximate the contact reduction, we use Google mobility data. We then compare the resulting
91 parameter estimates to a fit to a subset of pre-pandemic data and to a fit using an alternative
92 transmission forcing function. Finally, we investigate how two hypothetical vaccination strategies
93 may impact the regular seasonal pattern.

94 Methods

95 Data

96 We used two types of RSV data to inform our model parameters. The main data source was an
97 incidence times series from the respiratory diseases surveillance system in New South Wales
98 [27,28]. These reports comprise the weekly incidence of laboratory confirmed RSV and
99 influenza cases, as well as the total number of tested cases (influenza only). The data include
100 only symptomatic patients that sought healthcare and had a sample taken, which are an
101 unknown fraction of the total number of cases. RSV cases are defined as a patient for whom
102 RSV was detected by cell culture, nucleic acid testing (PCR), antigen testing or serology
103 (https://www1.health.gov.au/internet/main/publishing.nsf/Content/cda-surveil-nndss-casedefs-cd_rsv.htm). We included cases recorded between 8. January 2010 and 6. February 2022.
104 From 2015 - 2019 both the base levels and the amplitude of RSV notifications increased, which
105 coincided with an increasing number of samples tested for influenza in the same surveillance
106 network (see Figure S1a). However, emergency department visits for bronchiolitis remained
107 roughly the same between 2010-2019 with around 350 cases per week at peak seasonal
108 activity (Figure S1b) suggesting an increase in sensitivity of the sentinel surveillance rather than
109 an increasing burden of disease. The increase in testing was in part due to the introduction of
110 new multiplex PCR assays in some hospitals in 2015 [29]. Secondly, we used annual RSV
111 infection attack rates estimates from a longitudinal, prospective study in Kenyan households,
112 which collected biweekly samples of all participants regardless of symptoms [4]. The change in
113 contact patterns due to COVID-19 mitigation measures since early 2020 was approximated
114 through the Google Community Mobility index [30]. We selected the mobility index at
115 workplaces as most indicative of changes in RSV transmission relevant contacts besides
116 schools (which are not covered in the Google mobility data). We used the rolling 7-day median
117 index to smooth the data while retaining changing trends in mobility (Fig. S2a).
118

119 Model and parameter calibration

120 We developed a dynamic compartmental transmission model with sequential acquisition of
121 immunity (adapted from [6,14]) to account for the natural history of RSV infection. Briefly,
122 individuals are classed into five different states (S, E, I, R¹, R²) at four different levels (0,1,2,3+)
123 that reflect the number of previous RSV infections. The two R compartments at each level
124 correspond to an Erlang distributed duration of immunity [31]. Infants are born into the
125 susceptible compartment S₀ at a rate μ . When infected, they become latently infected (E₀) and
126 subsequently infectious (I₀) after which they become temporarily but fully immune (R₀¹ followed
127 by R₀²). After this temporary but sterilising immunity wanes, individuals become partially
128 susceptible again (S₁). Subsequent re-infection will lead to similar progression while keeping
129 track of the number of previous infections until an individual has had three infections, after which
130 infections are assumed to no longer lead to differences in immunity and susceptibility.
131 Susceptibility to re-infection and duration of infectiousness are assumed to decrease with repeat
132 exposure. The duration of the protective immunity was assumed to be the same at each level of
133 immunity. The population was modelled with a life expectancy of 80 years and a constant
134 birth/death rate μ , which results in a closed population of constant size. We assumed that the
135 effective per capita transmission rate (β_{eff}) varied seasonally due to seasonal differences in
136 contacts and pathogen viability in the environment. We modelled the seasonal forcing with a
137 modified Von Mises function (MVM) with parameter k that allows adjusting the variance of the
138 peak (see supplement). The MVM can take any shape between a cosine-like function and a flat
139 line with a sharp peak on a single day. The change in contact behaviour during the pandemic
140 was modelled by scaling the force of infection with a time-varying parameter i with $i \in [0, 1]$,
141 which was estimated from Google Community Mobility data [30] (see supplement).

142
143 We fitted the model jointly to the two datasets described above. We assumed that the reported
144 weekly incidence is a fraction ρ of the incident symptomatic cases, and that only cases of levels
145 0-2 would lead to severe enough disease requiring testing. The present surveillance data does
146 not provide age information but earlier laboratory data confirm that >93% of all tests were for
147 children aged <5 years old [32,33]. The reporting rate comprises the overall combined
148 probability of symptomatic disease, visiting a GP and having a sample taken and analysed by
149 the laboratory. To account for the non-linear increase in sampling and testing over time, we
150 assumed ρ followed a sigmoid function with two parameters: an initial reporting rate ρ_0 , and a
151 rate of increase, q (see supplement). For (2), we assumed an average level-specific attack rate
152 calculated as the cumulative cases at the end of the year divided by the population size at the
153 beginning of the year for a given level of reinfection. The model was fitted jointly to the reported
154 weekly incidence of cases assuming a Negative Binomial likelihood with dispersion parameter
155 ψ , and to the yearly attack rate data from a longitudinal Kenyan household study assuming a
156 Binomial likelihood (see supplement).

157
158 To improve the identifiability of all parameters and convergence, we fixed all parameters for
159 which we had acceptable point estimates and which did not depend on a specific geographical
160 setting to values from published literature. The following parameters of interest to the study
161 question were estimated: the baseline transmission rate (β_0), the amplitude (η), peak width (k)

162 and phase shift (ϕ) of seasonal transmission rate and the reduction of the susceptibility to
163 reinfection at the different levels ($\delta_1, \delta_2, \delta_3$) (Table 1). Moreover, we estimated the baseline and
164 rate of increase in the reporting rate (ρ_0 and q) and the dispersion parameter of the observation
165 model (ψ), since these depend on the data and cannot easily be compared between settings.
166 The proportion asymptomatic or the duration of infectiousness are often assumed to differ by
167 age and/or level of reinfection, but the latter is not commonly measured in observational studies.
168 We therefore converted age-specific estimates to level-specific estimates assuming that level 0
169 corresponds to age <1 year, level 1 to age 1-2 years, level 2 to age 3-5 years and level 3 to 5+
170 years.

171
172 The model was fitted with a Bayesian MCMC algorithm with the priors shown in Table 1. We
173 simulated the model with a run-in period of 100 years before evaluating the likelihood to ensure
174 a stable periodic orbit (quasi equilibrium). We used the Hamiltonian Monte Carlo (HMC) No-U-
175 Turn Sampler (NUTS) algorithm implemented in the Julia package Turing.jl [34,35] to run 10
176 chains with 500 iterations burn-in and 500 posterior samples per chain. Convergence was
177 confirmed with the Gelman-Rubin statistics (estimates <1.1 were considered indicative of
178 convergence). The uncertainty of model-derived quantities was calculated from the 2.5th and
179 97.5th percentile of all trajectories over each modelled data point (posterior predictive interval
180 PPI). Marginal posteriors are reported as median and 2.5th - 97.5th percentiles Credible
181 Intervals (CrI).

182 Sensitivity analysis

183 To explore the sensitivity of the model parameters to changes in the underlying data, we fit the
184 same model to a subset of the RSV incidence data covering only the pre-pandemic period
185 2010-2019, and compared the posterior cross-correlations and the marginal posterior
186 distributions. We also studied the effect of the choice of the seasonal forcing function on the
187 trajectory fit and the posterior parameter estimates in a sensitivity analysis. We re-fit the model
188 to the 2010-2022 data using a cosine forcing (see supplement), which has one parameter less
189 and produces a symmetric peak and nadir around an average transmission rate. The trajectory
190 fit was compared to the main results with the Von Mises forcing using Pareto-smoothed
191 importance sampling leave-one-out cross-validation (LOO) [36]. Finally, we omitted the Kenyan
192 attack rate data from the likelihood function and fitted the model with the Von Mises forcing only
193 to the time series data from NSW, and compared the results.

194 Vaccination strategies

195 To investigate how active immunisation of infants against RSV may interfere with RSV
196 seasonality, we used the posterior estimates to forward simulate the pattern of RSV seasonality
197 in NSW and its changes under two different vaccination strategies. We simulated both
198 continuous (year-round) and seasonal vaccination in previously unexposed, fully susceptible
199 individuals in level 0 as a proxy for vaccinating infants. The model equations are given in the
200 supplement. Seasonal vaccination was simulated with a time window of seven months during
201 RSV season (March-October), corresponding to the seven months of RSV season when

202 monoclonal antibodies are commonly administered in NSW [37]. For simplicity we assume that
203 eligible individuals who are in the exposed (E_0) or infected (I_0) state before vaccination would
204 not generate an additional immune response following vaccination but simply progress to the
205 next regular level of immunity. We also assume that the vaccine confers the same type and
206 duration of immunity as the first infection. A temporary, sterilising immunity has been observed
207 in trials for a live-attenuated vaccine in children [38] and a protein-based vaccine in adults [39]
208 From the simulated trajectories we summarised 1) the shift in peak activity, 2) the changes in
209 the amplitude and 3) the yearly percentage of cases averted compared to the baseline scenario
210 of no vaccination. The simulated effective vaccination coverage ranged from 10% to 100% in
211 10% steps. The effective coverage is to be interpreted as the product of distribution coverage
212 and vaccine effectiveness. We did not include the passive immunisation with monoclonal
213 antibodies in our model, which prevents severe disease but does not lead to sequential
214 acquisition of immunity. The number of infants receiving the currently licensed monoclonal
215 antibodies is small with respect to the total population of infants and we deem the effect of a
216 delayed susceptibility in these infants irrelevant for the transmission dynamics in our model.

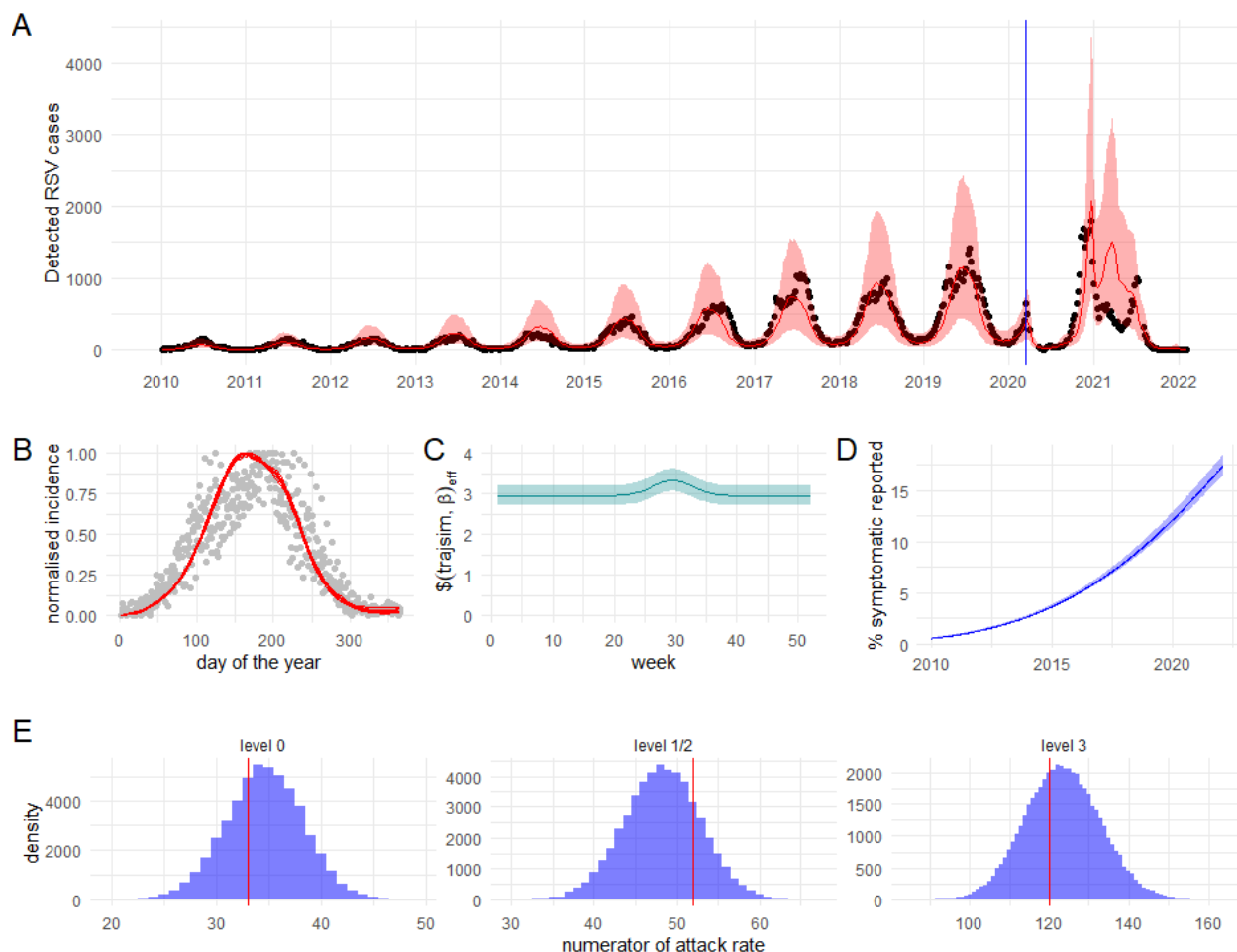
217 Results

218 RSV seasonality

219 In the 10 years prior to the COVID-19 pandemic, RSV in NSW commonly peaked mid-July
220 (median ISO week 28, range ISO week 18-32, i.e. May to August) with 66-79% of all annual
221 cases occurring during the five months between April and August (Fig. S1C). In 2020, the
222 beginning RSV season was abruptly terminated in March followed by a delayed peak in
223 December 2020 (6 months after the typical season) and a smaller regular peak in July 2021
224 (Fig. S1D).

225
226 The model was able to replicate the regular seasonal pattern, the increase in reported incidence
227 over time as well as the pandemic-related disruption with the exception of the first half of 2021,
228 where the model overestimated the reported cases (Fig. 1A & B). We estimated RSV
229 transmission to be high but only moderately seasonal with 2.94 (95% CrI 2.72-3.19) effective
230 contacts per day for most of the year and a narrow peak with a maximum of 3.33 (95% CrI 3.04-
231 3.69) effective contacts per day (13.1% increase above baseline, 95% CrI 12.7-13.6%) at week
232 29 at the end of July (Figure 1C). The average duration of sterilising, post exposure immunity,
233 the other determinant of regular seasonal RSV behaviour, was estimated as 412 days (95% CrI
234 391-434 days) (Table 1). We also estimated that 0.6% (95% CrI 0.5-0.6%) of symptomatic RSV
235 infections among levels 0-2 were reported through the sentinel surveillance in 2010, increasing
236 to 15.3% (95% CrI 14.5-16.2%) in 2022 (Fig. 1D). The level-specific attack rates were 63%
237 (95% PPI 60-66%), 59% (95% PPI 57-62%), 58% (95% PPI 56-61%) and 35% (95% PPI 33-
238 36%) for levels 0-3, respectively, which closely matches the attack rate data the model was
239 fitted to (Fig. 1E). Overall, we estimate that the average incidence was ~2.9 Million cases (95%
240 PPI 2.8-3 million) per year (36% of the population). MCMC trace plots, diagnostics and
241 additional numerical results are shown in the supplementary text and Figures S3A, S4A.

242



243

244

245 Fig. 1. Fitted model. The shaded areas represent the 95% posterior predictive intervals; the
246 darker lines represent the medians. A) Simulated trajectory fit and the weekly data points (black
247 dots). The blue vertical line denotes the first implementation of the lockdown measures in NSW.

248 B) The normalised fitted total incidence (red line) matches the normalised observed data (grey

249 grey dots) except for the peak timing, which is likely preceded by a few days. C) The fitted seasonal

250 transmission rate (β_{eff}) is large with a narrow peak in July and a maximum increase of 1.13

251 times the baseline. D) The fit also suggests an initial reporting rate of <1% of all symptomatic

252 cases in children increasing to 15% in 2022. E) The numerator of the attack rates as fitted by

253 the model (blue distribution) matched the data points (red line).

254

255

256

257

258

259

260 Table 1. Parameters used in the model. Values were either fixed from literature or fitted.
 261 U=Uniform(lower bound, upper bound), NT=normal truncated(mean, sd, lower bound, upper
 262 bound).
 263

Symbol	Parameter	Fixed mean value or prior	Posterior value Median (95% CrI)
β_0	Baseline transmission rate	Gamma(4.0, 1.0)	2.94 (2.73-3.19)
η	Amplitude of seasonal peak	U(0.0, 2.0)	0.39 (0.33-0.49)
k	Width scaling of seasonal peak	U(0.0, 3.0)	0.39 (0.29-0.48)
φ	Phase shift of seasonal transmission (days)	NT(180.0, 40.0, 0.0, 364.0)	202 (206-209)
ρ_0	Initial reporting rate	Beta(1.0, 30.0)	0.0056 (0.0051, 0.0061)
q	Increase in reporting rate	U(0.0, 0.001)	2.5*1e-4 (2.4-2.6)
ψ	Dispersion parameter of observation model	Beta(1.0, 30.0)	0.17 (0.15-0.19)
ω	Average duration of immunity (days)	NT(250, 125, 60, 730) [40,41]	412 (391-434)
δ_1	Scaling of susceptibility of secondary infection relative to primary	Beta(35.583, 11.417) [6]	0.83 (0.73-0.90)
δ_2	Scaling of susceptibility of tertiary infections relative to secondary	Beta(22.829, 3.171) [6]	0.93 (0.84-0.98)
δ_3	Scaling of susceptibility of subsequent infections relative to tertiary	Beta(6.117, 12.882) [6]	0.31 (0.28-0.36)
$1/\gamma_0, 1/\gamma_1$	Average duration of first infectiousness (days)	9.0	Fixed [42]
$1/\gamma_2$	Average duration of second and third infectiousness (days)	3.9	Fixed [42]
$1/\gamma_3$	Average duration of fourth and further infectiousness (days)	1.6	Fixed [42]
μ	Mortality and birth rate (per day)	1/(80*365)	Fixed
$1/\sigma$	Average duration of exposure (days)	4.0	Fixed [43]
p_0	Proportion asymptomatic at level 0	0.091	Fixed [4]
p_1, p_2	Proportion asymptomatic at level 1 and 2	0.173	Fixed [4]
p_3	Proportion asymptomatic at level 3	0.778	Fixed [4]

264 Sensitivity analysis

265 Fitting the same model to the pre-pandemic period (2010-2019) resulted in seemingly bimodal
266 posterior samples (Fig. S3B) due to two chains getting stuck in a local mode as suggested by
267 the log posterior plot (Fig S4B). For the estimation of the posterior predictive and the parameter
268 correlation we therefore excluded these two chains. The fit to the time series data was almost
269 identical to the result from the full dataset (Fig. S5A). However, several of the parameters that
270 govern seasonality, particularly the baseline effective transmission rate (β_0) and the amplitude of
271 the seasonal forcing (η) were highly positively correlated (Fig. S5B top) suggesting a poor
272 parameter identifiability. Including the pandemic period in the fit successfully reduced the
273 correlation among most of the parameters with the exception of a negative correlation between
274 η and k (which defines the width of the seasonal forcing) (Fig. S5B bottom). It's likely that the
275 model fits best with a specific area under the curve of the transmission rate during the season.
276 Fitting to the full data set also resulted in narrower and more informative posteriors (Fig S5C).

277
278 Our main findings of a low seasonal forcing for RSV were robust to the shape of the forcing
279 function. When the seasonal forcing was modelled with a cosine function, the model fitted the
280 data almost as well (expected log pointwise predictive density -3485.94) as with a Von Mises
281 function (ELPD -3413.37) but produced a larger uncertainty (S6A). The effective transmission
282 rate was slightly lower at the nadir (2.82, 95% CrI 2.64-3.02), and the amplitude (maximum over
283 minimum) was 1.10, which is a similarly weak seasonal forcing as with the Von Mises function
284 (1.13) (Fig. S6B). The posterior densities were similar for the two forcing functions (Fig. S6C).
285 However, the duration of immunity was estimated to be slightly shorter for the cosine model
286 (392 days, 95% CrI 371-414 days). Of note, the cosine model turned out to be more challenging
287 to fit. The majority of the chains did not converge within 48 hours and had to be cancelled,
288 which could mean the posterior samples we obtained (Fig S3C, Fig. S4C) may not be
289 representative of the target distribution.

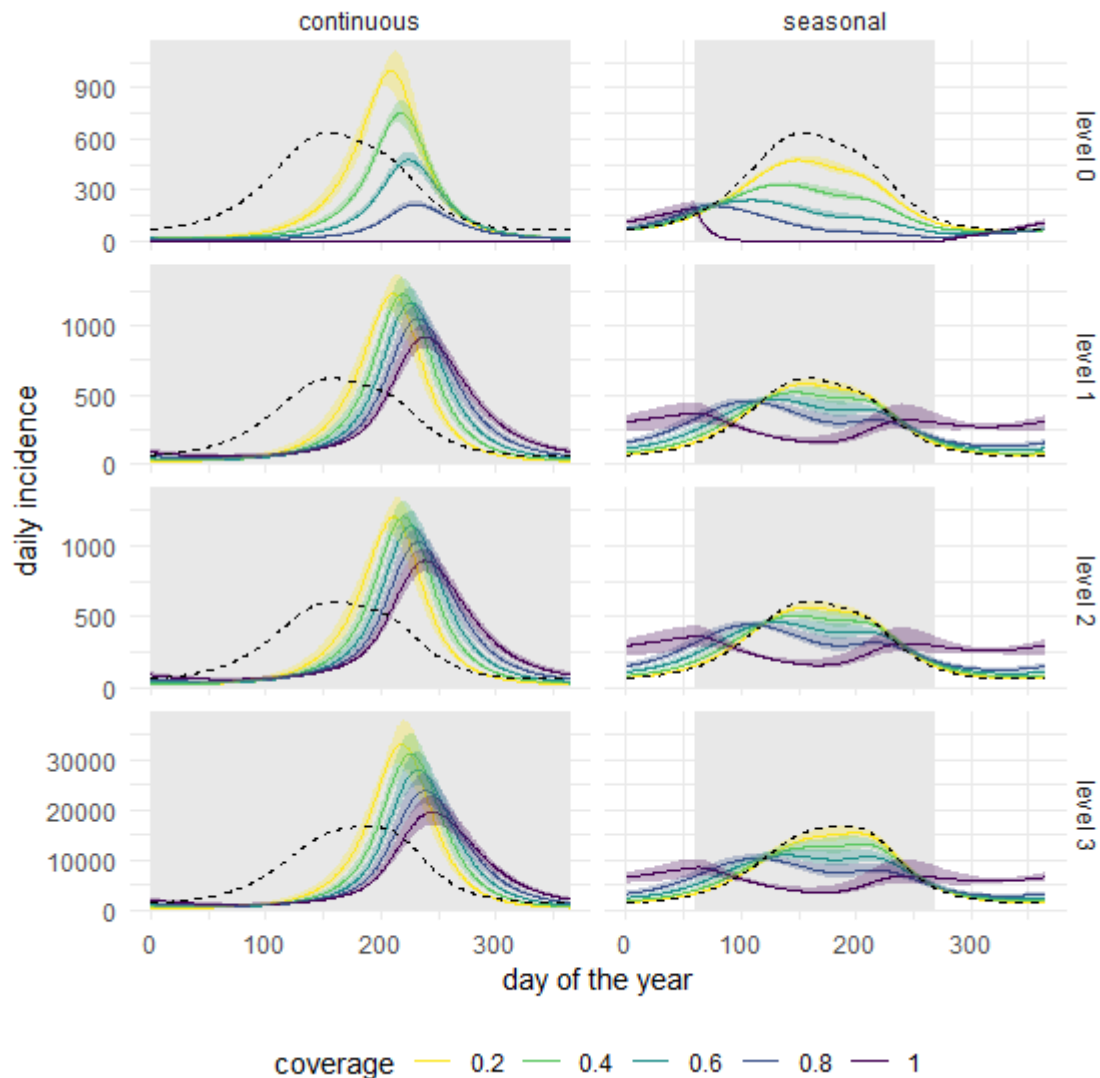
290
291 Fitting only to the time series data from NSW, omitting the Kenyan attack rate data, resulted in a
292 poorer chain mixing (including one chain stuck in a local mode) (Fig. S3D) and longer runtime,
293 which, when using HMC NUTS, is indicative of a more difficult posterior to sample from. The
294 trajectory fit was almost identical to the fit from the joint datasets (Fig. S7A), and the attack rates
295 predicted by the model for the levels 0-2 were similar (Fig S7B). However, the predicted attack
296 rates at level 3 were marginally higher when fitted without the AR data (median 41%, 95 % CrI
297 36-46%). Including the additional data for the attack rate led to more identifiable parameters (Fig
298 S7C) and narrower marginal posterior distributions for some parameters including the duration
299 of immunity (ω) (Fig. S7D). These results suggest that including the additional attack rate data
300 improved our inference framework.

301 Impact of vaccination strategies on seasonal pattern

302 We found that despite the relatively weak seasonal forcing, neither continuous (year-round) or
303 seasonal immunisation of infants is likely to disrupt RSV seasonality as substantially as the
304 COVID-19 pandemic did. Continuous vaccination is predicted to lead to delayed and more

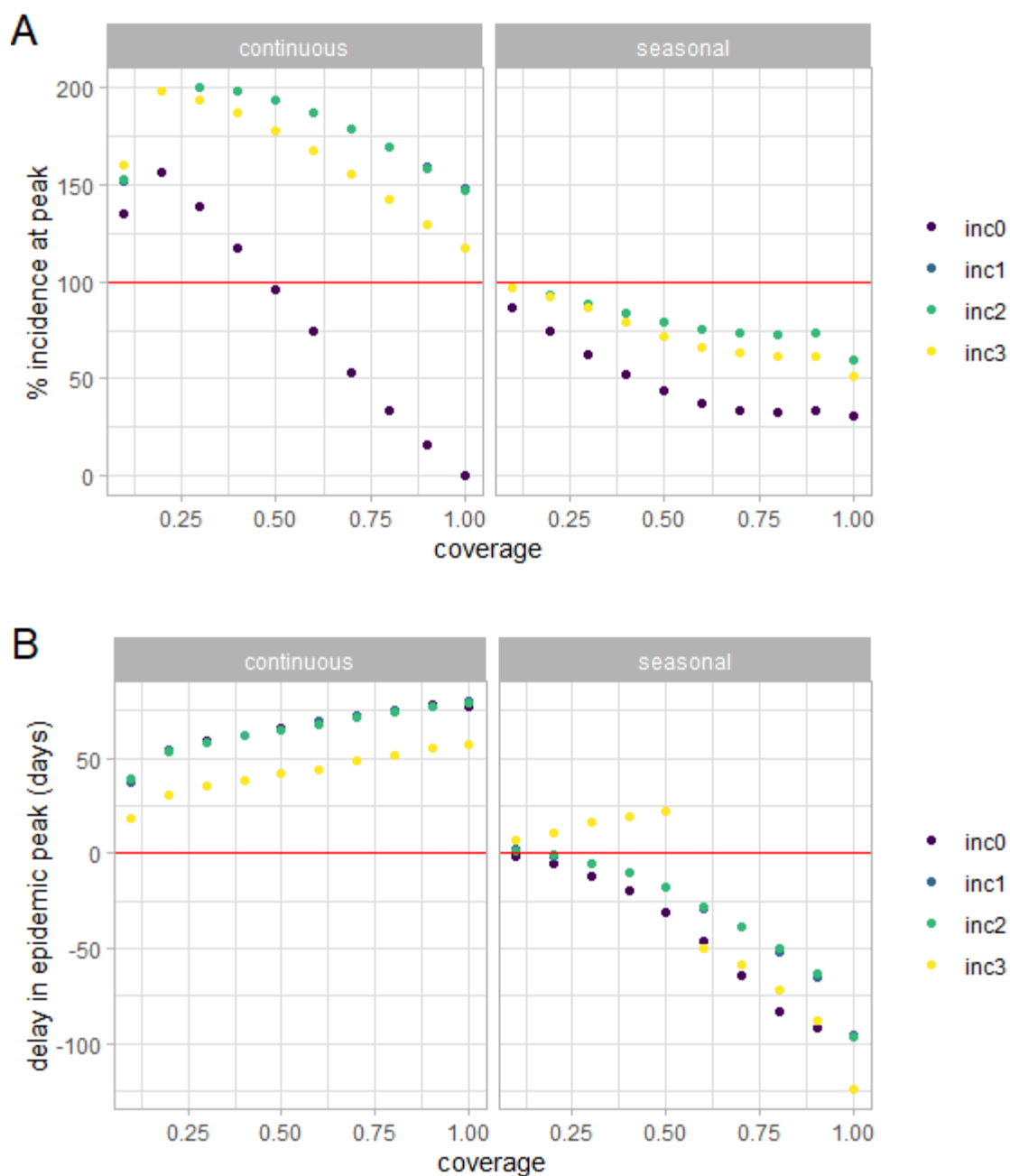
305 pronounced seasonal patterns with a narrower peak at all levels of (re-)infection (Fig. 2) with a
306 higher peak at lower coverages. Seasonal vaccination on the other hand flattened the seasonal
307 peak but increased the incidence off-season. Seasonal vaccination at 100% coverage led to a
308 weak bimodal pattern in those previously infected with a peak at the beginning and the end of
309 the regular season. Due to the more condensed season caused by continuous vaccination, the
310 infection incidence at peak can increase by up to 156% in the previously unexposed and up to
311 200% in previously exposed individuals if vaccine coverage is low (Fig. 3A). Only if vaccine
312 coverage exceeds 50% the peak incidence among previously uninfected decreases compared
313 to no vaccination. The peak timing is always delayed under a continuous strategy (Fig. 3B). The
314 delay increases with increasing vaccination coverage with a maximum delay of 80 days in the
315 previously exposed at 100% coverage. Seasonal vaccination also delays the peak at level 3 by
316 up to 17 days at low coverage, but generally advances the peak at all levels up to 129 days at
317 100% coverage. Both continuous and seasonal vaccination prevented a similar amount of cases
318 (Fig. 4). In the previously unexposed (level 0) the proportion of cases prevented increased
319 roughly linearly with increasing coverage and with only minimal displacement of infection and
320 disease into other groups (maximum 0.2%).

321



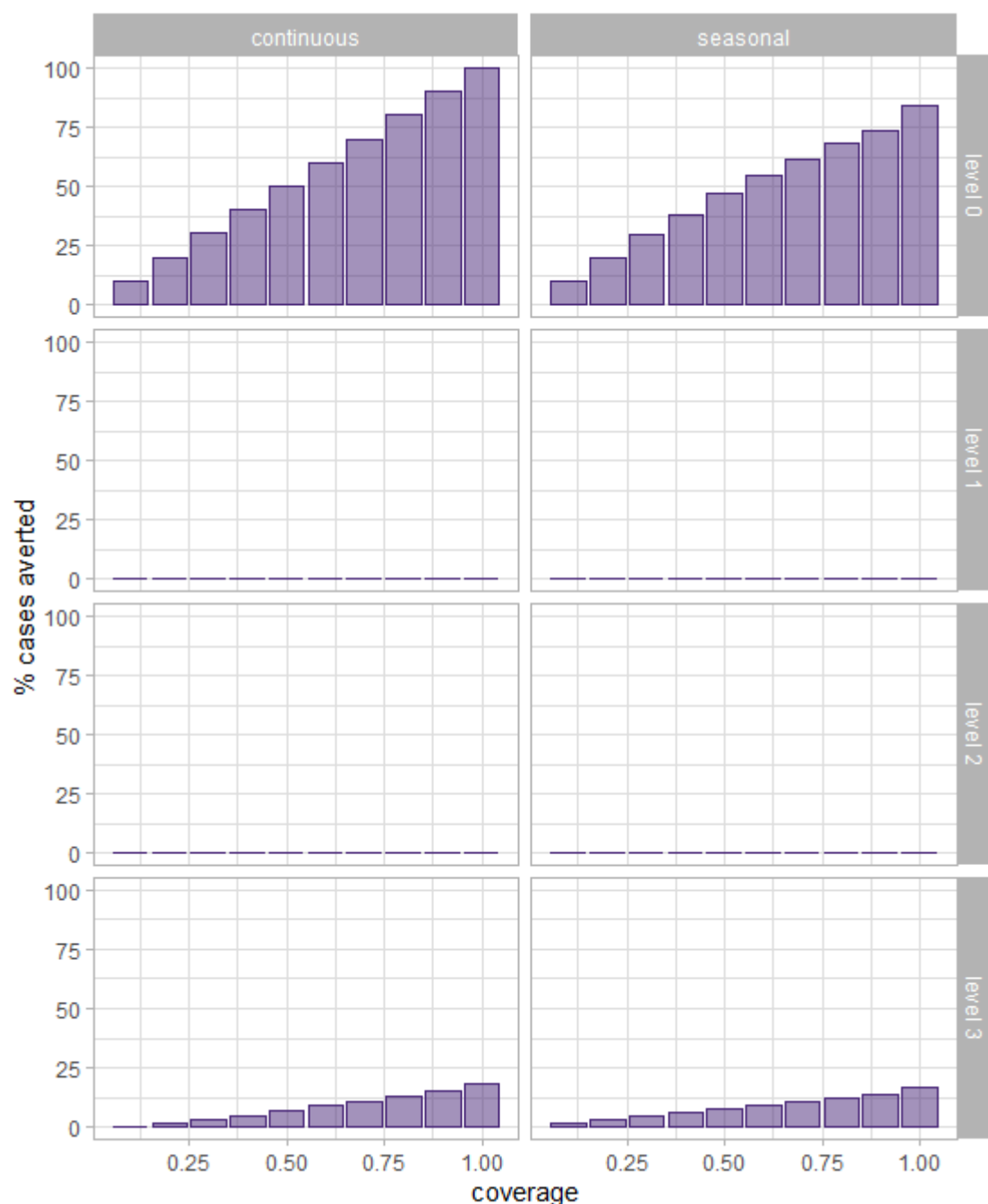
322
323

324 Fig. 2. Temporal changes in seasonal RSV incidence under different vaccination coverages and
325 strategies (seasonal vs. continuous, vaccination windows indicated by grey shaded areas)
326 compared to no vaccination (black dashed lines). Continuous vaccination leads to more narrow
327 epidemic peaks with larger amplitude and delayed peak timing at all levels for all coverages
328 (except 100% coverage at level 0). Seasonal vaccination at coverages less than 100% flattens
329 the epidemic peak at all levels. 100% seasonal coverage leads to two small peaks at the
330 beginning and the end of the regular season for levels 1-3.



331
332 Fig. 3. Quantitative effect of different vaccination coverages on peak timing and amplitude at all
333 levels (0-3). A) Percentage change of incident cases at peak relative to no vaccination.
334 Continuous vaccination increases the peak amplitude for level 0 if coverage is below 50%, and
335 for levels 1-3 regardless of coverage. Seasonal vaccination always decreases peak amplitude
336 B) Continuous vaccination delays the peak for all levels and coverages with a maximum of 80
337 days at coverage of 100%. Seasonal vaccination delays the peak for level 3 with a maximum of
338 17 days at a low coverage but otherwise advances the peak for all levels with a maximum of
339 129 days at 100% coverage.
340

341



342
343 Fig. 4. Percentage of cases averted by strategy for each level of (re-)infection. The prevention of
344 cases at levels 0 and 3 increases linearly with coverage, and continuous and seasonal
345 vaccination prevent almost the same percentage for a given coverage. Vaccination shifts more
346 fully susceptible individuals to level 2 than infection alone leading to a small increase in cases at
347 levels 1 and 2 at high coverage (maximum 0.2%, not visible on the graph).
348

349 Discussion

350 In this study, we show how pandemic disruptions of RSV can be used to quantify the factors
351 that drive the seasonal pattern. In a setting like NSW, the best fitting transmission rate is high
352 but mostly constant throughout the year with a single, narrow peak in winter with a maximum
353 amplitude of 1.13 times the minimum. Our sensitivity analysis confirmed our suspicion that fitting
354 only to the pre-pandemic time series resulted in an acceptable match to the time series data but
355 also in a correlation of the parameters governing seasonality. Excluding the attack rate data
356 also led to higher overall parameter correlation and less informative posteriors. When the
357 transmission rate was modelled as a cosine function, we could also obtain a similarly good fit to
358 the data as with the Von Mises function (albeit with a wider uncertainty) and similar posteriors.
359 However, the lower transmission rate was counteracted by a lower duration of immunity. The
360 low amplitude of seasonal forcing (maximum over minimum) estimated in both models (cosine
361 and Von Mises) suggests that moderate changes in contact rates and/or pathogen viability are
362 sufficient to trigger a seasonal peak. The amount of seasonal forcing estimated in other studies
363 is quite heterogeneous (ranging from 1.04 to 9.8 times the baseline [6,40,44–54], which may
364 suggest problems in the parameter inference but also geographical heterogeneity in the
365 seasonal transmission parameter. This also emphasises the need for more data resulting from
366 quantifiable disturbances of the regular RSV dynamics from other geographical settings to
367 narrow down the parameter space. Not only the seasonal forcing but also the average duration
368 of infection induced immunity in the literature - either as a fitted model parameter or estimated
369 from observational studies - varies substantially (range 169 - 744 days [6,40,44–46,48,49,51–
370 53]. Here we show that based on our model, the immunity may last longer than the ~250 days
371 suggested by Australian reinfection data [40]. The high force of infection and the resulting low
372 average age at first and second infection is also consistent with data from a longitudinal study
373 from Finland, which shows that ~60% of children under the age of three years were re-infected
374 every year [55].

375
376 Our simulation study shows that a strategy of continuous vaccination of previously unexposed
377 individuals can lead to a delayed and more extreme seasonal pattern (both among the
378 previously unexposed and the total population) particularly for low coverages. Continuous
379 vaccination reduces the pool of susceptibles (level 0) leading to a low level of RSV circulation.
380 When the total availability of susceptibles is large enough, a seasonal outbreak with a narrow
381 and large peak is possible. These potential changes in the amplitude and peak timing of RSV
382 following vaccination have practical implications for health services and public health strategies.
383 Even though year-round vaccination averts cases, it may lead to undesirable disease dynamics.
384 A large seasonal surge in paediatric cases as a result of low but continuous coverage could
385 lead to an excess of paediatric ICU admissions or attendances to other health services, which in
386 the worst case could result in higher paediatric mortality. Seasonal vaccination on the other
387 hand flattens the seasonal peak in our model at most coverages, which leads to more
388 manageable disease dynamics. However, the increase in off-season incidence would require
389 more year-round vigilance and adjusted testing guidelines in both infants and elderly.
390 On a more theoretical level, our results also underline the need to investigate the mechanistic
391 drivers of seasonality more in depth. In our model, the seasonal forcing of the transmission rate

392 (β_{eff}) can be interpreted as a function of the seasonally varying contact rate of people and the
393 seasonally varying probability of transmission upon contact. Our model fit suggests a narrow
394 peak of the seasonal forcing fits slightly better than a symmetric cosine-like behaviour for a
395 setting like NSW. Indoor contact rates are crucial for diseases transmitted via aerosols, and the
396 time spent indoors has a clear seasonal variation. The seasonality of indoor activities depends
397 on the climate zone. As shown by a recent study, seasonal indoor activity in the Southern USA
398 (which includes the same Köppen Geiger climate zone as NSW) showed a rather narrow peak
399 in Winter and did not fit well to a cosine function [56]. Further research to disentangle and
400 quantify the magnitude of seasonal contacts, partial host susceptibility, pathogen viability and
401 the association with seasonally-determined factors such as meteorological conditions, school
402 terms, time spent indoors and periodic social gatherings could provide further insight into the
403 seasonality of RSV, and lead to more identifiable and realistic model parameters tailored to
404 specific settings.

405
406 Our study has limitations and uncertainties. Firstly, our model is not age-structured, which
407 required us to make some simplifying assumptions about immunity and vaccination. In the
408 continuous vaccination strategy, we assume that the never exposed, vaccinated group are
409 babies who are vaccinated at birth. In the seasonal strategy, only those never exposed and
410 those currently infected are vaccinated. In practice, children who are immune after infection for
411 the first time cannot readily be identified as being immune without serology testing, and will
412 therefore likely also be vaccinated, which may or may not further improve their immunity and
413 decrease their susceptibility, which could influence the transmission dynamics at a population
414 level. The active immunisation of babies at birth is likely not feasible either, and year-round
415 vaccination will probably be done during routine check-ups in the first year of life. Our model
416 also does not consider maternal antibodies in new-borns, which provide some level of protection
417 during the first months of life. This type of passive immunisation depends on the number of
418 women that are pregnant in the last trimester and recovering from RSV. A more structured
419 model that includes age and differential contact patterns may be needed to adequately track
420 these numbers throughout the year. An age-structured model may also improve the prediction
421 of the incidence following vaccination because age-specific contact patterns give a better
422 approximation of the FOI than the infection-level specific FOI in our current model. Other factors
423 such as seasonal birth pulses [57] are known to influence the periodicity of childhood infectious
424 diseases, but the birth rate of NSW is remarkably constant throughout the year, and thus has
425 little to no impact on the seasonal RSV pattern in NSW. We also did not include the seasonal
426 migration of workers since we did not have access to migration data and do not know enough
427 about the mixing pattern with the general population.

428
429 Secondly, the data we use for parameter calibration have their limitations. The attack rate data
430 are taken from a prospective household study in Kenya where circulation of RSV may be
431 different from NSW. A prospective study in Australia showed an attack rate of 35% in 0-1 year
432 olds and 60% in 1-2 year olds [58]. The second estimate agrees well with the Kenyan data,
433 while 0-1 year olds seem more protected in Australia, possibly due to maternal antibodies,
434 which we have not modelled here. No data were available from Australia for older children or
435 adults. Limited data from various high income settings suggest that the symptomatic attack

436 rates in adults may be in the range of 3-11% [59–61], which - assuming that ~78% of adults are
437 asymptomatic [4] - corresponds roughly to an attack rate of 13-50%. A 20% overall attack rate
438 was observed among women participating in the placebo group of a clinical trial [62]. A better
439 understanding of the true level of circulation of RSV by age group and geographical setting
440 would improve not only our parameter estimation but also any predictions for vaccination
441 strategies. We also made some assumptions about the laboratory data, which represent only a
442 small and unknown fraction of all cases. The sigmoidal increase in detection and reporting is an
443 approximation we chose in the absence of the number of RSV tests performed. While the
444 sigmoid function seems to describe the pre-pandemic increase well, the reported RSV incidence
445 during the first half of 2021 was not matched very well by the model. It is conceivable that RSV
446 testing was reduced during the pandemic compared to 2019, but we could not quantify the true
447 time-varying underreporting with the type of data available to us. Additional seasonal variation in
448 reporting, e.g. increased detection of cases with disease exacerbation due to seasonal pollution
449 [63] or increased testing during RSV season because of a higher expectation, cannot be ruled
450 out. Additional data such as bronchiolitis emergency department visits, which are routinely
451 collected and reported and do not depend on changes in testing platforms, could help to further
452 narrow down the parameter estimates of our model.

453
454 Thirdly, Google Community Mobility data may not be the optimal proxy for the overall reduction
455 in contacts during the COVID-19 pandemic. A limited number of surveys conducted in Australia
456 between April and July 2020 showed that the average number of daily non-household contacts
457 in NSW were reduced by 70% during the initial phase and remained reduced by 25% in July
458 [64]. The fitted contact reduction based on these survey data correlates with the mobility
459 reduction, but the Google data may underestimate the actual reduction by up to 20% (Figure
460 S2b). To our knowledge, there are no data on the magnitude of contact reduction after July
461 2020 for Australia. In Germany, Google mobility data were found to correlate well with the
462 contact data collected in 2020 when weighted for home/non-home contacts [65]. A similar 1:1
463 correlation of the reduction of mobility at workplaces with the reduction of work contacts was
464 also found in the UK with the CoMix study (see Fig. S1 of [66]). Given the good correlation
465 found in these other studies and the lack of individual contact data for 2021, we considered the
466 Google Community Mobility data an acceptable proxy measure for modelling reduced
467 transmission. A better understanding of how contact rates related to mobility during the
468 pandemic in Australia would be helpful in narrowing down the posteriors and further improving
469 the fit during the pandemic phase. It is possible that the increase in mobility in 2021 compared
470 to the previous year is not a good indicator of an increase in effective contacts because of
471 continued measures such as mask wearing, and the mismatch between the model and the data
472 during the first half of 2021 is the result of poor correlation of mobility reduction and contact
473 reduction.

474
475 In conclusion, our study illustrates how the disruption of the seasonal pattern of endemic
476 infectious diseases following the COVID-19 NPIs can be used to quantify the factors that govern
477 seasonality. Immunisation strategies for RSV are unlikely to substantially alter the timing of RSV
478 season in Australia dramatically, but the type of vaccination strategy can influence the amplitude
479 of the seasonal incidence. However, these results may not hold for RSV transmission in climate

480 zones with a weaker seasonality, where the shifts in incidence might possibly be more
481 pronounced following the introduction of a vaccine.

482 Data availability

483 The R/Julia code as well as all input and output data are available in a Github repository
484 (<https://github.com/fkrauer/RSV-seasonality-public>). The original RSV case notification data are
485 available on the MSW MoH website [27,28]. The Google mobility data were downloaded from
486 [30].

487 Author contributions

488 **FK:** conceptualization, methodology, software, validation, formal analysis, data curation,
489 visualization, writing – original draft, writing – review & editing. **TEF:** methodology, software,
490 validation, writing – review & editing. **MK:** methodology, writing – review & editing. **DH:**
491 methodology, writing – review & editing. **MTS:** project administration, funding acquisition, writing
492 – review & editing. **CH:** data curation, writing – review & editing. **MJ:** conceptualization, funding
493 acquisition, writing – review & editing. **OW:** project administration, funding acquisition, writing –
494 review & editing. **TH:** project administration, funding acquisition, writing – review & editing. **SF:**
495 project administration, conceptualization, methodology, funding acquisition, supervision, writing
496 – review & editing.

497 Ethics

498 No ethical approval was needed as all data used were anonymised and publically available.

499 Funding

500 **FK:** Innovation Fund of the Joint Federal Committee (grant no. 01VSF18015), Wellcome Trust
501 (grant no. 221303/Z/20/Z). **TEF:** PhD funding received from Huawei Technologies Research &
502 Development (UK) Ltd. **MK:** Innovation Fund of the Joint Federal Committee (grant no.
503 01VSF18015). **DH:** National Institutes of Health (1R01AI141534-01A1). **MJ:** European Union's
504 Horizon 2020 research and innovation programme SC1-PHE-CORONAVIRUS-2020 - project
505 EpiPose (No 101003688), the NIHR HPRU in Modelling and Health Economics (grant code
506 HPRU-2019-NIHR200908) and the NIHR HPRU in Immunisation (grant code HPRU-2019-
507 NIHR200929). **SF:** Wellcome Trust (grant no. 208812/Z/17/Z).

508
509 The views expressed are those of the authors and not necessarily those of the United Kingdom
510 (UK) Department of Health and Social Care, the National Health Service, the National Institute
511 for Health Research (NIHR), the UK Health Security Agency or any other funder. The European
512 Commission is not responsible for any use that may be made of the information it contains.

513 Conflict of interest

514 None.

515 Acknowledgments

516 We thank Dr. Christopher Rackauckas, Dr. Seth Axen and the Julia language community on
517 Slack for technical advice.

518 References

- 519 1. Andeweg SP, Schepp RM, van de Kassteelle J, Mollema L, Berbers GAM, van Boven M.
520 2021 Population-based serology reveals risk factors for RSV infection in children younger
521 than 5 years. *Scientific Reports* **11**, 8953. (doi:10.1038/s41598-021-88524-w)
- 522 2. Glezen WP, Taber LH, Frank AL, Kasel JA. 1986 Risk of primary infection and reinfection
523 with respiratory syncytial virus. *Am J Dis Child* **140**, 543–546.
524 (doi:10.1001/archpedi.1986.02140200053026)
- 525 3. Ohuma EO, Okiro EA, Ochola R, Sande CJ, Cane PA, Medley GF, Bottomley C, Nokes DJ.
526 2012 The Natural History of Respiratory Syncytial Virus in a Birth Cohort: The Influence of
527 Age and Previous Infection on Reinfection and Disease. *American Journal of Epidemiology*
528 **176**, 794–802. (doi:10.1093/aje/kws257)
- 529 4. Munywoki PK, Koech DC, Agoti CN, Bett A, Cane PA, Medley GF, Nokes DJ. 2015
530 Frequent Asymptomatic Respiratory Syncytial Virus Infections During an Epidemic in a
531 Rural Kenyan Household Cohort. *J Infect Dis*. **212**, 1711–1718. (doi:10.1093/infdis/jiv263)
- 532 5. Mazur NI *et al.* 2018 The respiratory syncytial virus vaccine landscape: lessons from the
533 graveyard and promising candidates. *Lancet Infect Dis* **18**, e295–e311. (doi:10.1016/S1473-
534 3099(18)30292-5)
- 535 6. Hodgson D, Pebody R, Panovska-Griffiths J, Baguelin M, Atkins KE. 2020 Evaluating the
536 next generation of RSV intervention strategies: a mathematical modelling study and cost-
537 effectiveness analysis. *BMC Med* **18**, 348. (doi:10.1186/s12916-020-01802-8)
- 538 7. Treskova M, Pozo-Martin F, Scholz S, Schönfeld V, Wichmann O, Harder T. 2021
539 Assessment of the Effects of Active Immunisation against Respiratory Syncytial Virus (RSV)
540 using Decision-Analytic Models: A Systematic Review with a Focus on Vaccination
541 Strategies, Modelling Methods and Input Data. *Pharmacoeconomics* **39**, 287–315.
542 (doi:10.1007/s40273-020-00991-7)
- 543 8. Meijboom MJ, Rozenbaum MH, Benedictus A, Luytjes W, Kneyber MCJ, Wilschut JC, Hak
544 E, Postma MJ. 2012 Cost-effectiveness of potential infant vaccination against respiratory
545 syncytial virus infection in The Netherlands. *Vaccine* **30**, 4691–4700.
546 (doi:10.1016/j.vaccine.2012.04.072)

- 547 9. Obando-Pacheco P *et al.* 2018 Respiratory Syncytial Virus Seasonality: A Global Overview.
548 *J Infect Dis* **217**, 1356–1364. (doi:10.1093/infdis/jiy056)
- 549 10. Li Y *et al.* 2019 Global patterns in monthly activity of influenza virus, respiratory syncytial
550 virus, parainfluenza virus, and metapneumovirus: a systematic analysis. *The Lancet Global*
551 *Health* **7**, e1031–e1045. (doi:10.1016/S2214-109X(19)30264-5)
- 552 11. YUSUF S *et al.* 2007 The relationship of meteorological conditions to the epidemic activity
553 of respiratory syncytial virus. *Epidemiol Infect* **135**, 1077–1090.
554 (doi:10.1017/S095026880600776X)
- 555 12. Omer SB *et al.* 2008 Climatic, temporal, and geographic characteristics of respiratory
556 syncytial virus disease in a tropical island population. *Epidemiology & Infection* **136**, 1319–
557 1327. (doi:10.1017/S0950268807000015)
- 558 13. Pitzer VE, Viboud C, Alonso WJ, Wilcox T, Metcalf CJ, Steiner CA, Haynes AK, Grenfell BT.
559 2015 Environmental drivers of the spatiotemporal dynamics of respiratory syncytial virus in
560 the United States. *PLoS Pathog* **11**, e1004591. (doi:10.1371/journal.ppat.1004591)
- 561 14. Kinyanjui TM, House TA, Kiti MC, Cane PA, Nokes DJ, Medley GF. 2015 Vaccine Induced
562 Herd Immunity for Control of Respiratory Syncytial Virus Disease in a Low-Income Country
563 Setting. *PLoS ONE* **10**, e0138018. (doi:10.1371/journal.pone.0138018)
- 564 15. Baker RE, Mahmud AS, Wagner CE, Yang W, Pitzer VE, Viboud C, Vecchi GA, Metcalf
565 CJE, Grenfell BT. 2019 Epidemic dynamics of respiratory syncytial virus in current and
566 future climates. *Nat Commun* **10**, 5512. (doi:10.1038/s41467-019-13562-y)
- 567 16. Li Y, Wang X, Broberg EK, Campbell H, Nair H, Network ERS. 2022 Seasonality of
568 respiratory syncytial virus and its association with meteorological factors in 13 European
569 countries, week 40 2010 to week 39 2019. *Eurosurveillance* **27**, 2100619.
570 (doi:10.2807/1560-7917.ES.2022.27.16.2100619)
- 571 17. Jones N. 2020 How COVID-19 is changing the cold and flu season. *Nature* **588**, 388–390.
572 (doi:10.1038/d41586-020-03519-3)
- 573 18. Foley DA *et al.* 2021 The Interseasonal Resurgence of Respiratory Syncytial Virus in
574 Australian Children Following the Reduction of Coronavirus Disease 2019–Related Public
575 Health Measures. *Clinical Infectious Diseases* (doi:10.1093/cid/ciaa1906)
- 576 19. McNab S *et al.* 2021 Changing Epidemiology of Respiratory Syncytial Virus in Australia -
577 delayed re-emergence in Victoria compared to WA/NSW after prolonged lock-down for
578 COVID-19. *Clin Infect Dis* (doi:10.1093/cid/ciab240)
- 579 20. Tempia S *et al.* 2021 Decline of influenza and respiratory syncytial virus detection in facility-
580 based surveillance during the COVID-19 pandemic, South Africa, January to October 2020.
581 *Eurosurveillance* **26**, 2001600. (doi:10.2807/1560-7917.ES.2021.26.29.2001600)
- 582 21. Casalegno J-S *et al.* 2021 Characteristics of the delayed respiratory syncytial virus
583 epidemic, 2020/2021, Rhône Loire, France. *Eurosurveillance* **26**, 2100630.
584 (doi:10.2807/1560-7917.ES.2021.26.29.2100630)

- 585 22. Opek MW, Yeshayahu Y, Glatman-Freedman A, Kaufman Z, Sorek N, Brosh-Nissimov T.
586 2021 Delayed respiratory syncytial virus epidemic in children after relaxation of COVID-19
587 physical distancing measures, Ashdod, Israel, 2021. *Eurosurveillance* **26**, 2100706.
588 (doi:10.2807/1560-7917.ES.2021.26.29.2100706)
- 589 23. Agha R, Avner JR. 2021 Delayed Seasonal RSV Surge Observed During the COVID-19
590 Pandemic. *Pediatrics* (doi:10.1542/peds.2021-052089)
- 591 24. National Institute of Infectious Diseases (NIID). 2021 RSV Infection. See
592 <https://www.niid.go.jp/niid/en/10/2096-weeklygraph/1661-21rsv.html> (accessed on 22 July
593 2021).
- 594 25. Lumley SF *et al.* 2022 Changes in paediatric respiratory infections at a UK teaching hospital
595 2016–2021; impact of the SARS-CoV-2 pandemic. *Journal of Infection* **84**, 40–47.
596 (doi:10.1016/j.jinf.2021.10.022)
- 597 26. Coma E, Vila J, Méndez-Boo L, Antón A, Mora N, Fina F, Fàbregas M, Medina M. 2022
598 Respiratory Syncytial Virus Infections in Young Children Presenting to Primary Care in
599 Catalonia During the COVID-19 Pandemic. *J Pediatric Infect Dis Soc* **11**, 69–72.
600 (doi:10.1093/jpids/piab121)
- 601 27. NSW Health. 2012 Influenza Surveillance Reports 2012-2021. See
602 <https://www.health.nsw.gov.au/Infectious/Influenza/Pages/reports.aspx> (accessed on 9
603 February 2021).
- 604 28. NSW Health. 2020 COVID-19 weekly surveillance reports. See
605 <https://www.health.nsw.gov.au/Infectious/covid-19/Pages/weekly-reports.aspx> (accessed on
606 9 February 2021).
- 607 29. Wabe N, Lindeman R, Post JJ, Rawlinson W, Miao M, Westbrook JI, Georgiou A. 2021
608 Cepheid Xpert® Flu/RSV and Seegene Allplex™ RP1 show high diagnostic agreement for
609 the detection of influenza A/B and respiratory syncytial viruses in clinical practice. *Influenza
610 and Other Respiratory Viruses* **15**, 245–253. (doi:10.1111/irv.12799)
- 611 30. Google LLC. 2021 COVID-19 Community Mobility Report. *COVID-19 Community Mobility
612 Report*. See <https://www.google.com/covid19/mobility?hl=en> (accessed on 1 May 2022).
- 613 31. Camacho A, Ballesteros S, Graham AL, Carrat F, Ratmann O, Cazelles B. 2011 Explaining
614 rapid reinfections in multiple-wave influenza outbreaks: Tristan da Cunha 1971 epidemic as
615 a case study. *Proceedings of the Royal Society B: Biological Sciences* **278**, 3635–3643.
616 (doi:10.1098/rspb.2011.0300)
- 617 32. Lister S, McIntyre P, Menzies R. 2000 The epidemiology of respiratory syncytial virus
618 infections in NSW children, 1992–1997. *NSW Public Health Bull.* **11**, 119.
619 (doi:10.1071/NB00054)
- 620 33. Schindeler SK, Muscatello DJ, Ferson MJ, Rogers KD, Grant P, Churches T. 2009
621 Evaluation of alternative respiratory syndromes for specific syndromic surveillance of
622 influenza and respiratory syncytial virus: a time series analysis. *BMC Infectious Diseases* **9**,
623 190. (doi:10.1186/1471-2334-9-190)

- 624 34. Ge, Hong, Xu, Kai, Ghahramani, Zoubin. 2018 Turing: a language for flexible probabilistic
625 inference. pp. 1682–1690. Playa Blanca, Lanzarote, Canary Islands, Spain.
- 626 35. Xu K, Ge H, Tebbutt W, Tarek M, Trapp M, Ghahramani Z. 2020 AdvancedHMC.jl: A robust,
627 modular and efficient implementation of advanced HMC algorithms. In *Proceedings of The*
628 *2nd Symposium on Advances in Approximate Bayesian Inference* (eds C Zhang, F Ruiz, T
629 Bui, AB Dieng, D Liang), pp. 1–10. PMLR.
- 630 36. Vehtari A, Gelman A, Gabry J. 2017 Practical Bayesian model evaluation using leave-one-
631 out cross-validation and WAIC. *Stat Comput* **27**, 1413–1432. (doi:10.1007/s11222-016-
632 9696-4)
- 633 37. Xu R, Fathima P, Strunk T, de Klerk N, Snelling TL, Richmond PC, Keil AD, Moore HC.
634 2020 RSV prophylaxis use in high-risk infants in Western Australia, 2002-2013: a record
635 linkage cohort study. *BMC Pediatrics* **20**, 490. (doi:10.1186/s12887-020-02390-5)
- 636 38. Karron RA *et al.* 2005 Identification of a Recombinant Live Attenuated Respiratory Syncytial
637 Virus Vaccine Candidate That Is Highly Attenuated in Infants. *The Journal of Infectious*
638 *Diseases* **191**, 1093–1104. (doi:10.1086/427813)
- 639 39. Schmoele-Thoma B *et al.* 2021 High respiratory syncytial virus vaccine efficacy against
640 human challenge.
- 641 40. Moore HC, Jacoby P, Hogan AB, Blyth CC, Mercer GN. 2014 Modelling the Seasonal
642 Epidemics of Respiratory Syncytial Virus in Young Children. *PLoS ONE* **9**, e100422.
643 (doi:10.1371/journal.pone.0100422)
- 644 41. Hall CB, Douglas RG, Schnabel KC, Geiman JM. 1981 Infectivity of respiratory syncytial
645 virus by various routes of inoculation. *Infection and Immunity* **33**, 779–783.
646 (doi:10.1128/IAI.33.3.779-783.1981)
- 647 42. Hall CB, Geiman JM, Biggar R, Kotok DI, Hogan PM, Douglas GR. 1976 Respiratory
648 syncytial virus infections within families. *N Engl J Med* **294**, 414–419.
649 (doi:10.1056/NEJM197602192940803)
- 650 43. DeVincenzo JP *et al.* 2010 Viral Load Drives Disease in Humans Experimentally Infected
651 with Respiratory Syncytial Virus. *Am J Respir Crit Care Med* **182**, 1305–1314.
652 (doi:10.1164/rccm.201002-0221OC)
- 653 44. Acedo L, Díez-Domingo J, Morano J-A, Villanueva R-J. 2010 Mathematical modelling of
654 respiratory syncytial virus (RSV): vaccination strategies and budget applications. *Epidemiol.*
655 *Infect.* **138**, 853–860. (doi:10.1017/S0950268809991373)
- 656 45. Agoti CN, Mwiheri AG, Sande CJ, Onyango CO, Medley GF, Cane PA, Nokes DJ. 2012
657 Genetic Relatedness of Infecting and Reinfesting Respiratory Syncytial Virus Strains
658 Identified in a Birth Cohort From Rural Kenya. *The Journal of Infectious Diseases* **206**,
659 1532–1541. (doi:10.1093/infdis/jis570)
- 660 46. Hall CB, Walsh EE, Long CE, Schnabel KC. 1991 Immunity to and frequency of reinfection
661 with respiratory syncytial virus. *J. Infect. Dis.* **163**, 693–698. (doi:10.1093/infdis/163.4.693)

- 662 47. Hogan AB, Glass K, Moore HC, Anderssen RS. 2016 Exploring the dynamics of respiratory
663 syncytial virus (RSV) transmission in children. *Theoretical Population Biology* **110**, 78–85.
664 (doi:10.1016/j.tpb.2016.04.003)
- 665 48. Mahikul W, J. White L, Poovorawan K, Soonthornworasiri N, Sukontamarn P, Chanthavilay
666 P, F. Medley G, Pan-ngum W. 2019 Modeling household dynamics on Respiratory Syncytial
667 Virus (RSV). *PLoS ONE* **14**, e0219323. (doi:10.1371/journal.pone.0219323)
- 668 49. Mufson MA, Belshe RB, Orvell C, Norrby E. 1987 Subgroup characteristics of respiratory
669 syncytial virus strains recovered from children with two consecutive infections. *J Clin*
670 *Microbiol* **25**, 1535–1539.
- 671 50. Paynter S *et al.* 2014 Using mathematical transmission modelling to investigate drivers of
672 respiratory syncytial virus seasonality in children in the Philippines. *PLoS One* **9**, e90094.
673 (doi:10.1371/journal.pone.0090094)
- 674 51. Scott PD, Ochola R, Ngama M, Okiro EA, James Nokes D, Medley GF, Cane PA. 2006
675 Molecular analysis of respiratory syncytial virus reinfections in infants from coastal Kenya. *J*
676 *Infect Dis* **193**, 59–67. (doi:10.1086/498246)
- 677 52. Weber A, Weber M, Milligan P. 2001 Modeling epidemics caused by respiratory syncytial
678 virus (RSV). *Mathematical Biosciences* **172**, 95–113. (doi:10.1016/S0025-5564(01)00066-9)
- 679 53. White LJ, Waris M, Cane PA, Nokes DJ, Medley GF. 2005 The transmission dynamics of
680 groups A and B human respiratory syncytial virus (hRSV) in England & Wales and Finland:
681 seasonality and cross-protection. *Epidemiol. Infect.* **133**, 279–289.
682 (doi:10.1017/S0950268804003450)
- 683 54. White LJ *et al.* 2007 Understanding the transmission dynamics of respiratory syncytial virus
684 using multiple time series and nested models. *Math Biosci* **209**, 222–239.
685 (doi:10.1016/j.mbs.2006.08.018)
- 686 55. Kutsaya A, Teros-Jaakkola T, Kakkola L, Toivonen L, Peltola V, Waris M, Julkunen I. 2016
687 Prospective clinical and serological follow-up in early childhood reveals a high rate of
688 subclinical RSV infection and a relatively high reinfection rate within the first 3 years of life.
689 *Epidemiol Infect* **144**, 1622–1633. (doi:10.1017/S0950268815003143)
- 690 56. Susswein Z, Rest EC, Bansal S. 2022 Disentangling the rhythms of human activity in the
691 built environment for airborne transmission risk. (doi:10.1101/2022.04.07.22273578)
- 692 57. Martinez-Bakker M, Bakker KM, King AA, Rohani P. 2014 Human birth seasonality:
693 latitudinal gradient and interplay with childhood disease dynamics. *Proceedings of the Royal*
694 *Society B: Biological Sciences* **281**, 20132438. (doi:10.1098/rspb.2013.2438)
- 695 58. Takashima MD, Grimwood K, Sly PD, Lambert SB, Chappell KJ, Watterson D, Ware RS.
696 2021 Epidemiology of respiratory syncytial virus in a community birth cohort of infants in the
697 first 2 years of life. *Eur J Pediatr* **180**, 2125–2135. (doi:10.1007/s00431-021-03998-0)
- 698 59. Falsey AR, Hennessey PA, Formica MA, Cox C, Walsh EE. 2005 Respiratory Syncytial
699 Virus Infection in Elderly and High-Risk Adults. *New England Journal of Medicine* **352**,
700 1749–1759. (doi:10.1056/NEJMoa043951)

- 701 60. Korsten K *et al.* 2021 Burden of respiratory syncytial virus infection in community-dwelling
702 older adults in Europe (RESCEU): an international prospective cohort study. *Eur Respir J*
703 **57**. (doi:10.1183/13993003.02688-2020)
- 704 61. O'Shea MK, Ryan MAK, Hawksworth AW, Alsip BJ, Gray GC. 2005 Symptomatic
705 respiratory syncytial virus infection in previously healthy young adults living in a crowded
706 military environment. *Clin Infect Dis* **41**, 311–317. (doi:10.1086/431591)
- 707 62. Glenn GM *et al.* 2016 A Randomized, Blinded, Controlled, Dose-Ranging Study of a
708 Respiratory Syncytial Virus Recombinant Fusion (F) Nanoparticle Vaccine in Healthy
709 Women of Childbearing Age. *J Infect Dis* **213**, 411–422. (doi:10.1093/infdis/jiv406)
- 710 63. Nenna R *et al.* 2017 Respiratory syncytial virus bronchiolitis, weather conditions and air
711 pollution in an Italian urban area: An observational study. *Environ Res* **158**, 188–193.
712 (doi:10.1016/j.envres.2017.06.014)
- 713 64. Golding N *et al.* 2020 Estimating temporal variation in transmission of SARS-CoV-2 and
714 physical distancing behaviour in Australia Technical Report 4, update 29 July 2020. See
715 [https://www.doherty.edu.au/uploads/content_doc/Technical_report_4_update_29July2020.p](https://www.doherty.edu.au/uploads/content_doc/Technical_report_4_update_29July2020.pdf)
716 [df](https://www.doherty.edu.au/uploads/content_doc/Technical_report_4_update_29July2020.pdf) (accessed on 21 July 2021).
- 717 65. Tomori DV *et al.* 2021 Individual social contact data and population mobility data as early
718 markers of SARS-CoV-2 transmission dynamics during the first wave in Germany—an
719 analysis based on the COVIMOD study. *BMC Medicine* **19**, 271. (doi:10.1186/s12916-021-
720 02139-6)
- 721 66. Davies NG, Barnard RC, Jarvis CI, Russell TW, Semple MG, Jit M, Edmunds WJ. 2021
722 Association of tiered restrictions and a second lockdown with COVID-19 deaths and hospital
723 admissions in England: a modelling study. *The Lancet Infectious Diseases* **21**, 482–492.
724 (doi:10.1016/S1473-3099(20)30984-1)

725